Electrically tunable, room-temperature quantum-cascade lasers

Antoine Müller,[a] Mattias Beck,[b] and Jérôme Faist[c]
University of Neuchâtel, CH-2000 Neuchâtel, Switzerland

Ursula Oesterle[d] and Marc Ilegems[e]
Swiss Institute of Technology, CH-1015 Lausanne, Switzerland

(Received 10 May 1999; accepted for publication 17 July 1999)

Electrical tuning of two-section quantum-cascade lasers is systematically investigated as a function of temperature and optical power. In pulsed operation, the active region design exhibits a low threshold current density ($5.2\,\mathrm{kA/cm^2}$), a high peak (100 mW), and average (3 mW) powers at 300 K. The strong linear Stark tuning of the laser transition allows large tuning ranges of $40\,\mathrm{cm^{-1}}$, corresponding to a wavelength tune from 9.75 to 10.15 μm at 260 K for a peak optical output power of 10 mW. The tuning range is still $20\,\mathrm{cm^{-1}}$ at the same optical output power at $T=300\,\mathrm{K}$.
 [S0003-6951(99)04137-6]

There is a strong interest in the use of quantum-cascade (QC) lasers based on intersubband transitions[1] operating at room temperature in the midinfrared for sensing applications. Distributed feedback quantum-cascade lasers exhibit, even in pulsed operation, the narrow linewidth ($\Delta\nu \sim 0.1\,\mathrm{cm^{-1}}$) needed for atmospheric and low-pressure gas sensing applications.[2,3] The wavelength tunability offered by these devices ($\Delta\nu \sim 2-10\,\mathrm{cm^{-1}}$, Ref. 2), obtained by changing their temperature, is also sufficient for most of these applications. Spectroscopy of liquids or solids, on the other hand, do not usually require such narrow linewidth but at the same time require much broader tunability when, for example, one attempts the detection of a chemical in the presence of strong interference from other lines. Lead salt lasers would exhibit this wide tuning range by temperature tuning but at the cost of a cryogenic operation.[4] In this work, we demonstrated a QC laser based on an anticrossed diagonal active region whose wavelength can be strongly tuned electrically at room temperature.

As shown in Fig. 1, the active region of our structure is based on three quantum wells.[1,5–7] In this configuration, the radiative transition occurs between states $n=3$ and $n=2$ which have a reduced spatial overlap. For this reason, the transition energy is expected to vary linearly with the applied field through a first order Stark effect.[8,9] Our calculation of the transition energy as a function of the applied electric field confirms this expectation, as shown in Fig 1. In a previous published work, an even larger field tunability was observed at cryogenic temperatures in a structure based on a photon-assisted tunneling.[9] However, our structure is qualitatively different from this previous work because in our case both upper ($n=3$) and lower ($n=2$) state of the transition are anticrossed with the upper $n=4$, respectively, lower $n=1$ level.[5] This anticrossing reduces the field tunability of the laser transition but increases its oscillator strength, enabling very high performances at temperatures above room temperature to be achieved.[6,7] Note also that in our case, contrary to the work of Ref. 9, the laser action does not proceed by oscillator strength tuning because the lasing threshold is reached by increasing the upper state population.

The structure is grown by molecular-beam epitaxy using InGaAs and AlInAs alloys lattice matched on an InP substrate and consists of a 35 periods active region embedded in an optical waveguide similar to the one used in a previous work.[6] Square mesa etched samples were processed to study the field and temperature dependence of the luminescence spectrum. A summary of the results, whose details will be published elsewhere, are displayed in Fig. 1 where the energy of the luminescence peak is displayed as a function of the field for various temperatures. Surprisingly, the agreement between the calculated measured value of the tuning rate is better at room temperature than at 80 K. We do not have a good explanation for this surprising behavior that was not observed in the study of photon-assisted tunneling transition lasers.[9]

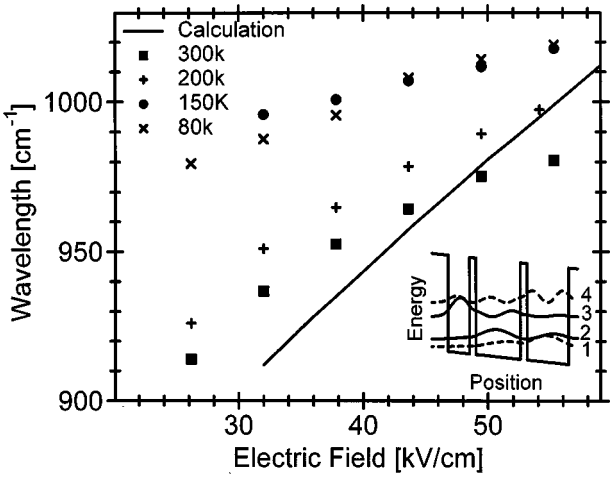

FIG. 1. Solid line: calculated transition energy as a function of applied electric field in the active region. Marks: Transition energy as a function of applied electric field measured for various temperatures. Inset: Schematic band structure of the active region.

[a]Also with: Alpes Lasers, rue Champréveyres 2, CH-2008 Neuchâtel, Switzerland; web site: www.alpeslasers.ch; electronic mail: Antoine.Muller@iph.unine.ch
[b]Electronic mail: Mattias.Beck@iph.unine.ch
[c]Electronic mail: Jerome.Faist@iph.unine.ch
[d]Electronic mail: Ursula.Oersterle@epfl.ch
[e]Electronic mail: Marc.Ilegems@epfl.ch

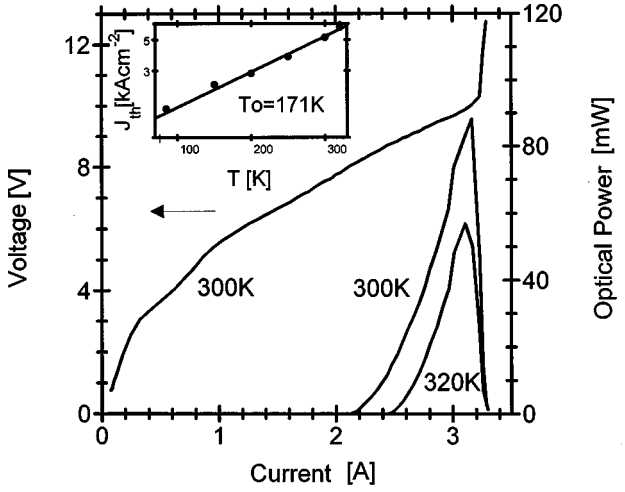

FIG. 2. Voltage measured at 300 K (left curve) and peak optical power measured at 300 and 320 K displayed as a function of injected current. The pulse duration is 100 ns and the repetition rate 5 kHz. The abrupt increase of the voltage and the concomitants decrease in optical power is due to a resonant tunneling effect. Inset: Threshold current density as a function of temperature.

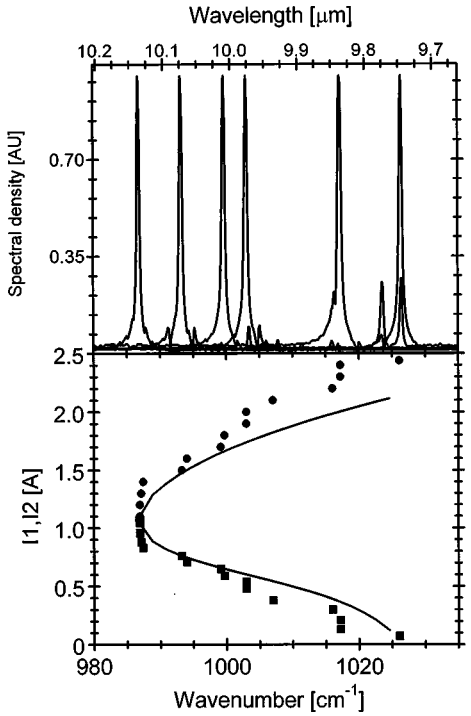

FIG. 3. Laser tuning at at $T-10$ C and constant optical power $P=5$ mW. (a) A few representative spectra for various currents. (b) Marks: currents in both sections for each tuning energy. Solid lines: prediction of the model.

The laser samples were processed into 28-μm-wide mesa etched ridge waveguides by wet etching across the active region, ZnSe passivation, and Ti/Au metallization. ZnSe has been chosen for its good optical properties allowing for lower waveguide losses than Si_3N_4. Figure 2 shows the peak optical power from a single facet versus the drive current for temperatures of $T=300$ and 320 K. The device was driven by 100 ns long pulses with a 5 kHz repetition rate. The average slope efficiency is $dP/dI=100\,\mathrm{mW/A}$ at $T=300\,\mathrm{K}$, with a maximum power of 90 mW at this temperature. The current is limited by resonant tunneling injection, as shown by the abrupt increase in voltage from 10 to more than 12 V at the maximum injection current (3.2 A). This behavior has been extensively discussed in a previous work.[5] In the inset of Fig. 2, the threshold current density Jth is plotted as a function of temperature. It has a value of only $5.2\,\mathrm{kA/cm^2}$ at 300 K. The data between ~ 100 and 320 K can be described by the usual exponential behavior $J\sim\exp(T/T_0)$ with an average $T_0\sim 170\,\mathrm{K}$. These data are reproducible across growth and processing runs, with a T_0 value always between 170 and 200 K. This weak dependence of the threshold current on the temperature is typical of the laser based intersubband transitions, especially those operating at long wavelengths. The output power and range of operating temperatures of this device are thus perfectly suitable for room-temperature spectroscopy. These devices have been also tested with a high duty cycle ($\sim 4\%$), the total output power being collected from one facet with a cone optics into a thermopile detector goes up to a maximum of 2–3 mW.

To enable the separate control of the emitted wavelength and optical power, the top contact metallization consists of two segments of equal length (750 μm), separated by a small gap. The resistance between two section (20 Ω) is much larger than the differential resistance of a single section (2 Ω), allowing us to inject different current densities J_1 and J_2 (Ref. 8). The total gain spectrum is now the sum of the two gain spectra of the individual sections. In this way, the value of the peak gain *and* its location can be controlled. Moreover, it can easily be shown that the tuning is continuous for sections of equal lengths.

In Fig. 3, the tunable operation of a 1.5-mm-long laser with two sections of equal lengths is displayed. The measurement was performed in pulsed operation, with 100 ns long pulsed at a 5 kHz repetition rate. The temperature was set at $T=260\,\mathrm{K}$. For this measurement, the current I_1 in the first section was set to some value. The current I_2 in the second section was then increased until a fixed amount of power (5 mW in Fig. 3) was obtained. A few representative spectra for various injected currents pairs are displayed in Fig. 3(a). For these low powers, the spectra are limited to a few (one or two) longitudinal modes of the Fabry–Perot cavity. The mode jumps between the different spectra reflect the continuous tuning of the gain curve. Some longitudinal modes do not appear, however. This behavior, already observed in the tuning of Fabry–Perot QC laser operating in continuous wave, is attributed to defects in the waveguide which will force a mode selection by slightly varying the loss of each individual mode. The total tuning range is $40\,\mathrm{cm^{-1}}$, which represents a relative tuning of $\Delta\nu/\nu$ of about 4%. The two drive currents I_1 and I_2 as a function of emitted photon energy are displayed for the same measurement in Fig. 3(b), along with the results of a simplified theoretical model. In the latter, the two gain spectra of the individual sections are assumed to have a Gaussian line shape with a full width at half maximum of 15 meV as measured from the electroluminescence data. We assumed a linear dependence of the transition energy with applied voltage (as given by the experimental data of Fig. 1) and a linear dependence of the peak gain on current. The value of the gain coefficient is inferred from the measurement of the waveguide loss ($40\,\mathrm{cm^{-1}}$) of the device by the analysis of the subthreshold

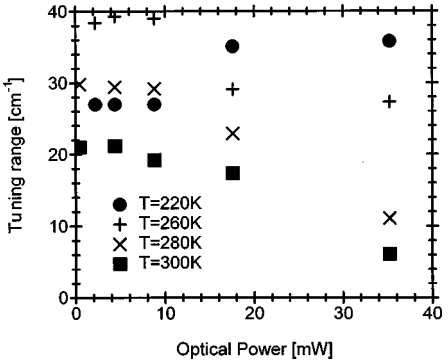

FIG. 4. Maximum tuning range as a function of the optical power and temperature.

luminescence and the value of the threshold current density. We also assumed a linear I–V relationship in the current range in which the laser would be tuned with a differential specific conductance of $\sigma_b = 1.34\,10^3\,\Omega^{-1}\,\mathrm{cm}^{-2}$ obtained from the experimental data of Fig. 2. The radiative component of the current is neglected, which is a good approximation at those low powers. As shown in Fig. 3, the model slightly underestimates the current needed for the section driven by the highest current. We attribute this discrepancy to gain saturation which is not included in our model.

Tuning is then studied systematically as a function of power and temperature. The results are displayed in Fig. 4. Let us note that at this temperature, the tuning range reaches the theoretical maximum, given simply by

$$\Delta\nu_{\max} \cong \frac{d\nu}{dV}\frac{J_0}{\sigma_d},$$

where J_0 is the threshold current density for a homogenously pumped structure, σ_d is the differential conductance per unit area, and $d\nu/dV = 1.3\,[\mathrm{mev/V}]$ the tuning rate of the transition is given by the slope of the characteristics of Fig. 1. The laser reaches its maximum tuning range $\Delta\nu_{\max}$ when it is able to operate on one section only, the other one being switched off. The tuning range at $T = 300\,\mathrm{K}$ and 4.2 mW is still of $30\,\mathrm{cm}^{-1}$. The decrease of the tuning range with an increasing temperature above 260 K is relatively easy to explain. Because the maximum current that may be injected in the device is weakly dependent of temperature,[5] the reduction of the gain coefficient with increasing temperature (with translates into a increase of the threshold current) reduces the maximum gain that can be reached in the device and therefore limits its tuning range. The reduction of the tuning range for temperatures lower than 260 K is caused by the reduction of the tuning rate of the active region $d\nu/dV$ shown by the luminescence data and an increase of σ_d.

Besides the large tuning obtained by shifting the gain curve, fine tuning of the individual Fabry–Perot longitudinal modes can be further performed if, for example, a narrow molecular absorption line has to be reached by varying the device temperature. Indeed, measurements of distributed feedback QC lasers made of the same material show that temperature tuning of the individual modes will occur at a rate $(1/\lambda)(\Delta\lambda/\Delta T) = 5\times10^{-5}$. For our device which displays a mode spacing of $1/2n_{\mathrm{eff}}L = 1.04\,\mathrm{cm}^{-1}$, this translates into a temperature difference of $+/-10°$.

As it is demonstrated in this work, electrical tuning of the gain curve is fairly straightforward to implement in a structure based on intersubband transitions. Because of their similar designs, this tuning should also be observed in GaAs-based QC lasers.[10] However, in general, interband semiconductor lasers[11] do not tune easily because the active region is based on a direct (type I) transition between electron and hole sates, which experience a weaker second-order Stark shift. In addition, the electric field in the active region of a *p-n* junction under direct injection is by definition very small. A notable exception would be asymmetric single heterojunction[12] or cascaded heterojunction interband lasers[13] based on type II transitions.

The authors would like to thank T. Aellen for processing some of the device used in this work. This work was supported by the Ministry for Education and Science (OFES) through the European project UNISEL under the Contract No. CT97-0557.

[1] J. Faist, F. Capasso, D. L. Sivco, C. Sirtori, A. L. Hutchinson, and A. Y. Cho, Science **264**, 553 (1994).
[2] J. Faist, C. Gmachl, F. Capasso, C. Sirtori, D. L. Sivco, J. N. Baillargeon, A. L. Hutchinson, and A. Y. Cho, Appl. Phys. Lett. **70**, 2670 (1997); C. Gmachl, J. Faist, F. Capasso, C. Sirtori, D. L. Sivco, J. N. Baillargeon, A. L. Hutchinson, and A. Y. Cho, IEEE Photonics Technol. Lett. **9**, 1090 (1997).
[3] K. Namjou, S. Cai, E. A. Whittaker, J. Faist, C. Gmachl, F. Capasso, D. L. Sivco, and A. Y. Cho, Opt. Lett. **23**, 219 (1998).
[4] M. Tacke, Infrared Phys. Technol. **36**, 447 (1995).
[5] C. Sirtori, F. Capasso, J. Faist, A. L. Hutchinson, D. L. Sivco, and A. Y. Cho, IEEE J. Quantum Electron. **QE–34**, 1722 (1998).
[6] J. Faist, C. Sirtori, F. Capasso, D. L. Sivco, J. N. Baillargeon, A. L. Hutchinson, and A. Y. Cho, IEEE Photonics Technol. Lett. **10**, 1100 (1998).
[7] C. Gmachl, A. Tredicucci, F. Capasso, A. L. Hutchinson, D. L. Sivco, J. N. Baillargeon, and A. Y. Cho, Appl. Phys. Lett. **72**, 3130 (1998); S. Slivken, A. Matlis, C. Jelen, A. Rybaltowski, J. Diaz, and M. Razeghi, *ibid.* **74**, 173 (1999).
[8] Y. J. Mii, K. L. Wang, R. P. G. Karunasiri, and P. F. Yuh, Appl. Phys. Lett. **56**, 1046 (1990); C. Sirtori, F. Capasso, D. L. Sivco, A. L. Hutchinson, and A. Y. Cho, *ibid.* **60**, 151 (1992).
[9] J. Faist, F. Capasso, C. Sirtori, D. L. Sivco, A. L. Hutchinson, and A. Y. Cho, Nature (London) **387**, 777 (1997).
[10] C. Sirtori, P. Kruck, S. Barbieri, P. Collot, J. Nagle, M. Beck, J. Faist, and U. Oesterle, Appl. Phys. Lett. **73**, 3486, (1998).
[11] ''Quantum Well Lasers,'' edited by P. S. Zory (Academic, San Diego, 1993).
[12] M. P. Mikhailova, I. A. Andreev, K. D. Moiseev, I. N. Timchenko, and Y. P. Yakovlev, Proceedings of the International Symposium on Nanostructures, St. Petersburg, Russia, 20–24 July 1994.
[13] R. Q. Yang, B. H. Yang, D. Zhang, C.-H. Lin, S. J. Murry, H. Wu, and S. S. Pei, Appl. Phys. Lett. **71**, 2409 (1997).